Regional Externalities of Clinker Production: Estimating Spatial Spillover Effects of Clinker Production on Air Pollution in Germany

Master Thesis Presented to the

Department of Economics at the

Rheinische Friedrich-Wilhelms-Universität Bonn

In Partial Fulfillment of the Requirements for the Degree of

Master of Science (M.Sc.)

Supervisor: Dr. Imke Rhoden

Submitted in October 2025 by:

Nargiz Ahmadova

Matriculation Number: 3290592

Table of Contents

1. Introduction

Air pollution represents one of the most pressing environmental challenges of the century, with industrial emissions being a significant contributor. Among industrial sectors, the cement industry is recognized as a major source of air pollution, contributing substantially to emissions of nitrogen oxides (NO_x), sulfur oxides (SO_x), and dust (Nwogu et al., 2025). In cement manufacturing, clinker-producing factories emit substantially higher primary air pollutants into the atmosphere than their non-clinker producing counterparts (Firdissa et al., 2024).

In Germany, there are 53 cement plants, among which 33 are involved in clinker production (Zementwerke, V.D., 2023). In 2022, these facilities generated approximately 32.9 million tonnes of cement and 23.2 million tonnes of clinker (Zementwerke, V.D., 2023). According to the German Informative Inventory Report (2022), during the clinker burning stage, 0.5 kg of NOx and 0.25 kg of SO2 are emitted for every ton of clinker produced. That means, in 2022, clinker production in Germany emitted around 11.6 kt of NOx and 5.8 kt of SOx. These figures underscore the importance of examining the contribution of clinker production to air pollution in Germany.

Emissions from clinker plants may not only affect the immediate area but also spill over into adjacent regions. A body of literature demonstrates the spatial autocorrelation of air pollutants (Dai and Zhou, 2017; Wu et al., 2022). These studies suggest that pollution levels in one region are not independent of those in neighboring areas. Hence, this paper analyzes not only the direct effects of clinker production on air quality but also its spatial spillover effects across regions in Germany.

2. Literature Review

My thesis topic is inspired by the work of Li et al. (2020), who studied the spatial spillover effects of cement production on air pollution in China. In their study, the authors use panel data of 30 provinces in China to examine direct and indirect impacts of cement production on air pollution. Using the Spatial Durbin Model (SDM), the authors indicate the presence of significant spatial spillover effects of cement production on air pollution, with the spillover effects exceeding the direct effects.

Beyond cement production, other strands of the literature also examine the spillover effects on air pollution. For instance, Zhao and Wang (2022) and Ding and Liu (2023) investigate the spatial spillover effects of urbanization, while Li et al. (2018) and Zhao et al.(2020) study how industrialization impacts pollution in the adjacent areas. Feng et al. (2020)

investigate the spillover effects of environmental regulation on air pollution, while Ma et al. (2016) examine how regional economic activities contribute to PM 2.5 emissions in adjacent regions. These studies collectively provide empirical evidence of significant spatial spillover effects.

The most used spatial econometric models in applied research are Spatial Lag Model (SLM), Spatial Error Model (SEM), and Spatial Durbin Model (SDM) (Tao and Yang, 2014). SDM has become particularly popular in literature. Several studies, including Zhao and Wang (2022), Li et al. (2018), Ding and Liu (2023), Feng et al. (2020), and Li et al. (2020) have used SDM to disentangle the direct and spillover effects on air pollution. Meanwhile, Zhao et al. (2020) use all three specifications (SLM, SEM, and SDM), while Ma et al. (2016) employ the SLM framework in their studies.

LeSage and Pace (2009) suggest that the selection of a spatial model should be made based on the likelihoods of different models, while the analysis should start from a more general model. Several studies (Li et al., 2020, Li et al., 2018) have followed this strategy. Essentially, these authors start with SDM and then test if the model needs to be degraded to SLM or SEM based on the results of Wald and likelihood ratio (LR) tests. In line with this approach, the present study also applies this 'general to special' framework.

3. Clinker Production and Air Pollution in Germany

3.1 Clinker Production within the Cement Manufacturing Process[1]

All over the world, cement is a critical component for the construction sector. The primary raw materials for making cement are limestone, clay, and marl (EMEP/EEA, 2023). Firstly, these ingredients are crushed and blended to form the raw meal (see Figure 1). The raw meal is then fed into a preheater tower, where it is heated before entering the kiln. In the final stage, the raw meal is heated at around 1450°C, a process called calcination (Heidelberg Materials). During calcination, the limestone (calcium carbonate) breaks down into lime (calcium oxide) due to the intense heat and this lime then combines with the other raw materials that together form clinker (Heidelberg Materials). After cooling, the clinker is ground together with gypsum and other additives, resulting in the final product—cement.

[1] The description refers to the production of Ordinary Portland Cement (OPC), which represents the standard type of cement worldwide. Other cement types may involve variations in raw materials or processing steps.

Figure 1: Cement Production Process Flow

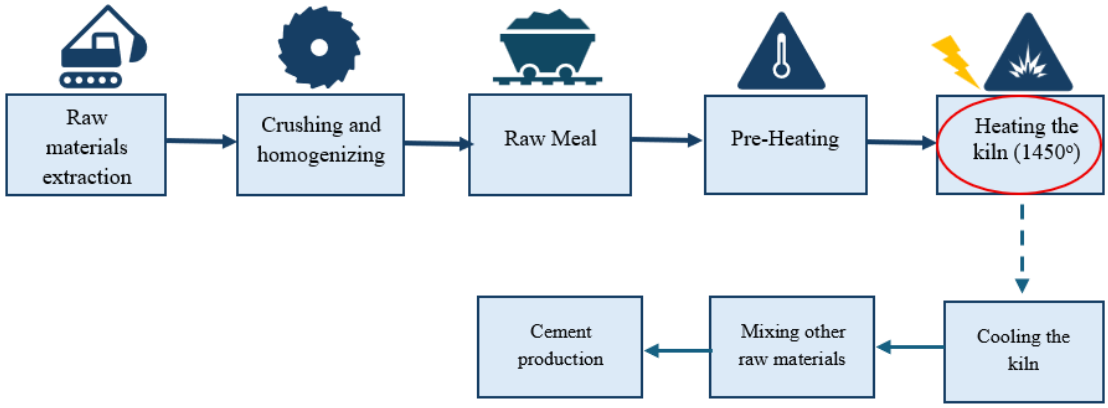

Source: Own illustration based on information provided by CEMBUREAU, 2024.

As the primary component of cement, clinker is also the main source of pollution in the manufacturing process (Ntziachristos et al., 2017). As marked with a red circle in Figure 1, the kiln heating stage for clinker formation represents the most emission-intensive step in the process. The extremely high temperatures needed to produce clinkers cause physical and chemical reactions of raw materials and fuels, which in turn release significant amounts of emissions into the atmosphere (EMEP/EEA, 2023). Nitrogen oxide (NO_x) is the main pollutant emitted from the kiln, followed by sulfur oxide (SO_x), dust and volatile organic compounds (EMEP/EEA, 2023).

Given the dominance of NO_x among clinker production pollutants, this paper adopts NO_x as a pollution indicator. Since most nitrogen oxides (NO_x) are converted into nitrogen dioxide (NO_2) in the atmosphere, emission data are reported as NO_2 per cubic meter (Zementwerke, V.D., 2023). Accordingly, the paper uses NO_2 concentrations as the measure of air pollution.

3.2 Spatial Distribution of Air Pollution in Germany

NO_2 is a significant air pollutant that poses serious risks to both human health and the environment. Exposure has been linked to various diseases, including lung function impairment (Jiang et al., 2019) and an increased risk of mortality from pulmonary heart disease (Chen et al., 2019).

In Figure 2a, we can see a choropleth map of Germany displaying average NO_2 concentrations across NUTS-3 regions in Germany in 2022. As illustrated by the map, the western regions of Germany exhibit significantly higher NO_2 concentrations compared to the

eastern regions. Notably, the highest concentrations are clustered in the Rhine–Ruhr metropolitan region in North Rhine–Westphalia, with additional hotspots along the Rhine corridor. In addition, Berlin appears as a distinct eastern hotspot.

By contrast, the lowest NO_2 levels are concentrated in northeastern Germany, particularly in Mecklenburg–Vorpommern, Brandenburg (outside Berlin), Schleswig-Holstein, and large parts of Lower Saxony and Saxony-Anhalt. Central Germany also shows a lower level of pollution in terms of nitrogen dioxide levels.

Figure 2. a) NUTS 3 level average NO_2 in Germany in 2022 b) Country level average NO_2 over 2018-2022

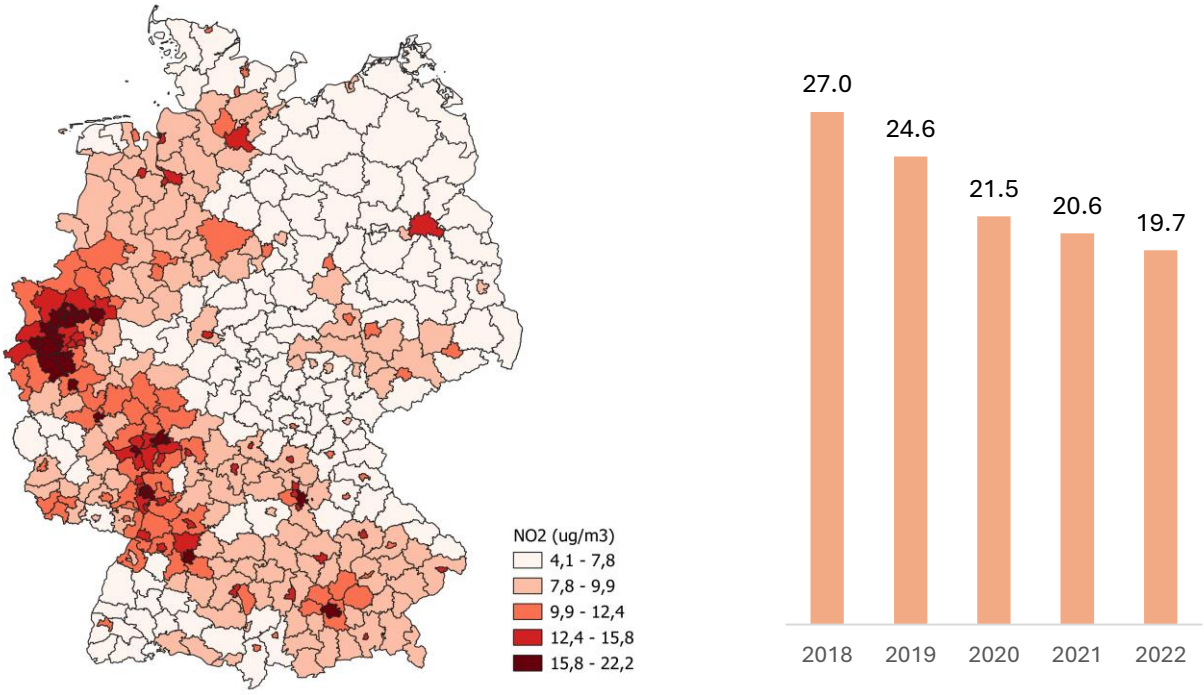

Source: Own illustration based on data by European Environment Agency, 2022

In Figure 2b, we can observe the declining trend in average NO_2 levels in Germany from 2018 to 2022. There has been a consistent decline in nitrogen dioxide levels, with a 27% decrease from 2018 to 2022. Among other drivers, this decline can be attributed to mobility and activity restrictions during the COVID-19 pandemic.

Spatial autocorrelation can be defined as the positive or negative correlation of a variable with itself due to the spatial location of the observations (Salima and Bellefon, 2018). Such spatial dependence can be due to the factors that are unobservable or difficult to quantify (Salima and Bellefon, 2018). The presence of spatial dependence in Germany can be statistically assessed using various techniques, among which Moran's I, Geary's C, and spatial autoregression are the most widely applied (Shekhar and Xiong, 2007). In this paper, I employ

Moran's I index, one of the earliest methods developed for measuring spatial autocorrelation (Moran, 1950), which remains the standard tool today.

The Global Moran's statistics measure spatial dependence by comparing each location's value with those of its neighbors. In essence, it calculates the mean of all observations, subtracts this mean from each value to obtain deviations, and then multiplies the deviations of neighboring pairs to form cross-products. A positive cross-product indicates that neighboring values are either both above or both below the mean, suggesting spatial clustering. Conversely, a negative cross-product indicates that one value is above and the other below the mean, which suggests spatial dispersion. In short, a positive and significant index indicates spatial clustering, whereas a negative and significant index indicates spatial dispersion. The null hypothesis for Moran's I index states that the values are randomly distributed across space, so if the index is not significant, it means the data do not provide evidence against randomness.

In this study, Global Moran's I is applied to nitrogen dioxide data. In addition to the standard test, a permutation-based Moran's I is performed to reduce errors that may result from the choice of spatial weights and from possible violations of the test's underlying assumptions. (Bivand et al., 2018). In both the standard and permutation-based tests, Moran's I was positive and significant at the 1% level across all years. Table 1 below presents the results.

Table 1. Moran's I results for 2018-2022

Year	Global Moran's I (NO_2)	p-value
2018	0.64	0.001
2019	0.65	0.001
2020	0.65	0.001
2021	0.65	0.001
2022	0.88	0.001

Positive and significant indices indicate that we can reject the null hypothesis that NO_2 is randomly distributed across Germany. In other words, the statistics indicate that NO_2 concentrations tend to be spatially clustered in Germany.

We can also visualize the Moran scatter plot in Figure 3, where NO_2 concentrations are on the horizontal axis and their spatial lag values are on the vertical axis. Spatial lag values are constructed by the average value of neighboring observations. Basically, for each region spatial lag value is calculated as the average value of the concentrations in the neighboring areas. Neighbors for each region are defined if they share either a border (edge) or a corner (vertex). All values are transformed to have a mean of zero.

Figure 3. Moran scatter plot of NO_2 in Germany, 2022

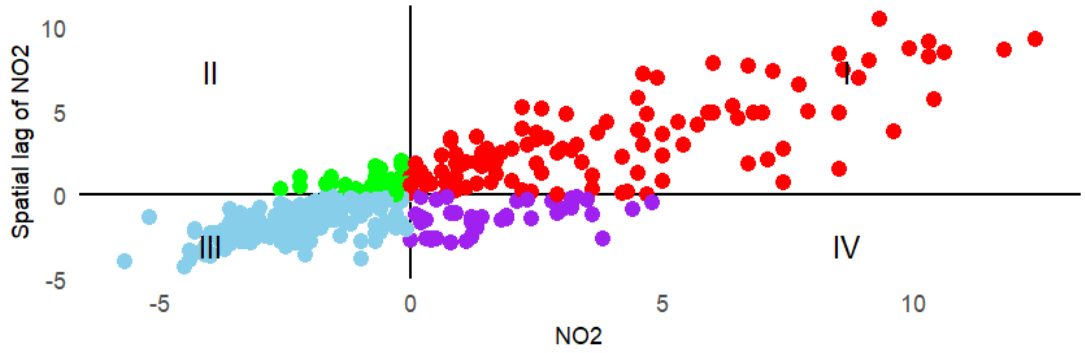

The scatter plots reveal a positive spatial association between regional pollutant levels and those of neighboring areas. For instance, points in Quadrant I represent regions where pollution levels are above the mean, and the average pollutant levels in surrounding regions are also above the mean—indicating spatial clustering of high values. Similarly, Quadrant III includes regions with below-mean pollution levels, surrounded by neighbors that also exhibit low pollution—suggesting clustering of clean areas. Conversely, quadrant II and quadrant IV represent the regions where spatial dispersion is pronounced. We can see that the majority of the points lie on quadrants I and III, indicating spatial clustering of pollutant levels in Germany.

4. Data

4.1. Selection of Variables

The unit of observation in this study is the NUTS-3 region in Germany. Germany is divided into 400 NUTS-3 regions, corresponding to districts (Kreise) and independent cities (kreisfreie Städte) (Eurostat, 2025). Due to data availability, 393 regions[2] are included in the analysis. Excluded regions are not involved in clinker production. The study period spans the years 2018 to 2022.

The dependent variable is the average concentration of nitrogen dioxide, measured in micrograms per cubic meter (ug/m^3).

The key explanatory variable in this study is clinker production, estimated from CO_2 emissions of clinker plants using an emission intensity factor. This factor is obtained by dividing total clinker production in Germany by total CO_2 emissions from cement production. The respective figures are taken from the international report by Schneider and Behrouzi (2023). Once the emission intensity factor for clinker production is obtained (0.81), it is multiplied by

[2] Excluded regions: DEB21, DE211, DE222, DE913, DE942, DE94H, DEB34

CO_2 emissions of individual clinker plants to get the total clinker produced by each plant. Plant-level emission data is provided by VDZ.

The selection of independent variables is important to isolate the effect of clinker production. Based on the literature review, this paper selects eight control variables. Three of these variables are GDP per capita (Li et al., 2020), population density (Zhao and Wang, 2022) and proportion of industrial value added (Li et al., 2020; Li et al., 2018; Thürkow et al., 2023). To test the Environmental Kuznets Curve (EKC) hypothesis in the German context, both GDP per capita and its squared terms are used.

According to the study by Thürkow et al. (2023), road transport is the largest contributor to nitrogen dioxide pollution in urban areas in Germany. To account for this sector, two control variables are included. The first captures the vehicle fleet composition through the number of petrol and diesel passenger cars. The second variable is traffic-related accidents, serving as a proxy for traffic volume because direct traffic volume data on a county level is not available.

Li et al. (2020) include internal expenditure of scientific research funds as a control variable for air pollution. Based on my research, no such data is available for counties in Germany, so this study uses an alternative measure, the percentage of socially insured employees working in knowledge and research-intensive industries at the place of work.

Thürkow et al. (2023) show that the combustion of coal, gas, solid biomass, and liquid fuels in private households is a significant source of nitrogen oxides in Germany. This implies that the household energy consumption structure is an important determinant of NO_2 pollution. However, data on the share of renewable energy use by households are not available at the county level. As a proxy, this study uses the share of newly completed residential buildings with renewable heating systems as the control variable.

Meteorological conditions can also influence air pollution. Shen et al. (2021) show that higher NO_2 concentrations are generally associated with lower wind speeds. Based on my research, wind speed data are not available for Germany at the county level. Therefore, following the methodology of Angelova and Lupio (2020), this study derives county-level yearly wind speed estimates from daily grid data (25 km × 25 km) provided by the Joint Research Centre of the European Commission.

The variable labels used in the regression models, along with their definitions, units, and sources of data are presented table 2 below.

Table 2. Variable settings

Variable	Definition	Data source	Unit
Pollution	Average NO_2 concentrations	European Environment Agency	ug/m3
Clinker	Amount of clinker production	VDZ	ton
gdp	Per capita GDP (base period=2010)	Eurostat	Euro
PopDens	Population Density	INKAR	Inhabitants per km²
Ind	Proportion of industrial value added in total value added	Eurostat	%
Cars	Petrol and diesel passenger cars, scaled by population	The Kraftfahrt-Bundesamt	per 1000 inhabitants
Rd	Share of employees in knowledge and research-intensive industries (workplace based)	INKAR	%
Wind	Average yearly wind speed	Joint Research Centre of the European Commission	Meter per second
RenHeat	Percentage of completed residential buildings with renewable heating energy in newly constructed residential buildings	INKAR	%
Traffic	Total road traffic accidents per 100,000 inhabitants	INKAR	per 100,000 inhabitants

4.2. Transformation of variables

Previous studies examining spillover effects have employed logarithmic transformations on variables to reduce estimation errors arising from heteroscedasticity and multicollinearity (Zhao and Wang, 2022; Li et al., 2020; Li et al., 2018). Following the same approach, all variables in this study are log-transformed, except for those expressed as percentages.

Since the clinker production data contains many zeros (24 out of 393 regions have clinker production), a standard log transformation cannot be applied. Some studies address the issue of zeros by adding a small positive constant to variables before applying the log transformation (e.g., log (x+1)). However, according to N'guessan et al. (2017), the arbitrary choice of 'small' positive numbers can affect the model results. To address this limitation, the inverse hyperbolic sine (asinh) transformation is used in this study. This transformation offers two key advantages: it can be used without any arbitrary manipulation of the original variable (Aihounton and Henningsen, 2021), while still allowing a similar interpretation of the coefficients as the log transformation (Bellemare and Wichman, 2020). The transformation is defined as follows:

$$\text{asinh}(x)=\ln(x+\sqrt{x^2+1})$$

5. Methodology

5.1 Model Construction

The existence of spatial dependence (see Section 3) in nitrogen dioxide necessitates the use of spatial econometric models, as traditional regression approaches may lead to the biased and inconsistent estimates (Anselin 1988, p.59). This arises because 'independent samples' assumption in the conventional econometric models is violated under spatial dependence (Zhao and Wang, 2022).

However, spatial econometric models effectively address the bias and inconsistency in coefficient estimates, thereby improving model accuracy and the reliability of statistical inference (Li et al., 2018). As discussed in Section 2, this paper adopts 'general to special' test method to select the appropriate spatial model.

First, the Spatial Durbin Model was estimated, and then whether it could be further simplified to the Spatial Lag Model or Spatial Error Model was judged based on the Likelihood Ratio (LR) test. For clarity, the equations of all three models are presented below.

The SLM contains the spatial lag term of air pollution that captures spatial autocorrelation, shown in Eq(1).

$$ln(Pollution_{it}) = a_0 + \rho W ln(Pollution_{it}) + \beta_1 asinh(Clinker_{it}) + \beta_2\, ln(gdp_{it}) + \beta_3\, ln(gdp_{it})^2 + \beta_4\, ln(PopDens_{it}) + \beta_5\, Ind_{it} + \beta_6 ln(Cars_{it}) + \beta_7 ln(Traffic_{it}) + \beta_8 Rd_{it} + \beta_9 RenHeat_{it} + \beta_{10} ln(Wind_{it}) + u_{it} \quad (1)$$

Since spatial dependence may also arise from omitted variables or unobserved shocks that are spatially correlated, Spatial Error Model is estimated, which incorporates a spatially lagged error term, shown in Eq (2) and (3).

$$ln(Pollution_{it}) = a_0 + \beta_1\, asinh(Clinker_{it}) + \beta_2\, ln(gdp_{it}) + \beta_3\, ln(gdp_{it})^2 + \beta_4 ln(PopDens_{it}) + \beta_5 Ind_{it} + \beta_6 ln(Cars_{it}) + \beta_7\, ln(Traffic_{it}) + \beta_8 Rd_{it} + \beta_9 RenHeat_{it} + \beta_{10} ln(Wind_{it}) + u_{it} \quad (2)$$

$$u_{it} = \lambda W u_{it} + \varepsilon_{it} \quad (3)$$

The Spatial Durbin Model (SDM) extends the spatial lag specification by including spatially lagged explanatory variables, thereby allowing both the dependent variable and the regressors to generate spatial spillover effects across regions, as shown in Eq (4).

$$ln(Pollution_{it}) = a_0 + \rho W ln(Pollution_{it}) + \beta_1\, asinh(Clinker_{it}) + \beta_2\, ln(gdp_{it}) + + \beta_3\, ln(gdp_{it})^2 + \beta_4\, ln(PopDens_{it}) + \beta_5\, Ind_{it} + \beta_6 ln(Cars_{it}) + \beta_7\, ln(Traffic_{it}) + \beta_8 Rd_{it} + \beta_9 RenHeat_{it} + \beta_{10} ln(Wind_{it}) + \varphi_{it}\, WX_{it} + \varepsilon_{it} \quad (4)$$

5.2. Model Selection

To decide whether SDM can be reduced to SLM or SEM models, the likelihood ratio tests are used. Based on the test, the SDM model provides a significantly better fit than the SAR model (LR = 559.38, $p < 0.001$), indicating that including spatially lagged explanatory variables substantially improves model performance. Similarly, the SDM model significantly outperforms the SEM model (LR = 46.77, $p < 0.001$), indicating that the spatial lag of explanatory variables explains the data more than what is captured by spatially correlated error terms alone. I additionally estimate the Spatial Durbin Error Model (SDEM), in the robustness checks, to incorporate spatial lag of error terms as well.

4 different specifications of SDM are conducted to control unobserved heterogeneity.

- No Fixed Effects (Pooled SDM): This is the baseline model without any fixed effects. It assumes that all spatial units and time periods share a common intercept.
- Time Fixed Effects: This specification controls for unobserved shocks common to all districts in a given year (e.g., a pandemic) by including year-specific intercepts.
- Spatial Fixed Effects: This model includes spatial fixed effects (on a NUTS-2 level) to capture time-invariant unobserved characteristics of the region such as geography.
- Two-Way Fixed Effects: This specification includes both time and spatial fixed effects to control both the region-specific and year-specific unobserved heterogeneity.

This paper uses a queen contiguity definition, where two regions are considered neighbors if they share (1) a common border or (2) a common vertex. Another commonly used spatial weight matrix is the inverse distance matrix, where the weight between two regions is calculated as the inverse of the distance between their centroids (1/d).

The main reason for this choice is that several independent cities in Germany (*kreisfreie Städte*) are geographically located entirely within a surrounding district. In such cases, the centroid-to-centroid distance becomes extremely small, which leads to disproportionately large weights in the inverse distance calculation. For example, in the case of Spree-Neiße, the weight between Spree-Neiße and the kreisfreie Stadt Cottbus is 0.56, while the next-highest weight, assigned to a bordering district, is only 0.048. This sharp contrast arises from the very short centroid-to-centroid distance between Cottbus and Spree-Neiße, because Cottbus is located within Spree-Neiße. However, air pollution disperses across borders easily as well, so such a large disparity between weights does not realistically capture the neighborhood structure relevant for pollution spillovers. Indeed, another paper (Rüttenauer, 2018) studying spatial spillover effects of environmental pollution in Germany uses a queen-based spatial weight

matrix. However, as a common practice, the model is also estimated using an inverse distance weight matrix, with the corresponding results presented in the robustness check section.

6. Results

Table 3 reports the estimated direct, indirect, and total impacts of the models, along with key model diagnostics and spatial correlation parameter (ρ). The corresponding coefficient estimates from the regression summaries are reported in Appendix.

Table 3. Direct, Indirect and Total Effects from SDM

	Baseline	Time FE	Spatial FE	Time & Spatial FE
R-squared	0.791	0.854	0.887	0.906
Adjusted R-squared	0.789	0.853	0.883	0.903
$Sigma^2$	0.022	0.013	0.012	0.009
Log-likelihood	4036.027	4070.746	4142.257	4178.012
pho (ρ)	0.889***	0.817***	0.838***	0.731***
AIC	–8028.05	–8099.49	–8166.51	–8240.02
BIC	–7905.22	–7982.24	–7837.10	–7916.19
Direct Effects				
asinh(Clinker)	0.004**	0.004***	0.005***	0.005***
ln(gdp)	-1.396***	-0.986***	-0.663**	-0.584**
$ln(gdp)^2$	0.068***	0.049***	0.033**	0.030**
ln(PopDens)	0.191***	0.193***	0.193***	0.191***
Ind	0.001***	0.001**	0.002***	0.001**
ln(Cars)	0.084***	0.120***	0.109***	0.115***
ln(Traffic)	0.045***	0.012	0.059***	0.008
Rd	-0.001*	-0.002***	-0.002***	-0.002***
RenHeat	-0.0003**	-0.0003	-0.001***	-0.0003*
ln(Wind)	-0.184***	-0.160***	-0.186***	-0.160***
Indirect (spillover) Effects				
asinh(Clinker)	0.034**	0.023**	0.032**	0.021***
ln(gdp)	-9.575**	-3.203***	-0.967	-0.960
$ln(gdp)^2$	0.469**	0.166***	0.056	0.059*
ln(PopDens)	0.273***	0.214***	0.236***	0.176***
Ind	0.006*	-0.0001	0.007*	-0.0004
ln(Cars)	0.553**	0.657***	0.283	0.132
ln(Traffic)	0.351***	-0.054	0.386***	-0.095
Rd	-0.006	-0.01***	-0.013**	-0.008***
RenHeat	-0.006***	-0.001	-0.010***	-0.001
ln(Wind)	-0.178	-0.164*	0.371**	0.113
Total Effects				
asinh(Clinker)	0.038**	0.024**	0.036**	0.026***
ln(gdp)	-10.971**	-4.302***	-1.630	-1.544
$ln(gdp)^2$	0.537**	0.22***	0.089	0.089*
ln(PopDens)	0.465***	0.406***	0.429***	0.367***
Ind	0.008*	0.002	0.008**	0.0004
ln(Cars)	0.637**	0.744***	0.392	0.248
ln(Traffic)	0.396***	-0.027	0.445***	-0.087
Rd	-0.007	-0.012	-0.015***	-0.010***
RenHeat	-0.006***	-0.001*	-0.011***	-0.001
ln(Wind)	-0.363**	-0.332***	0.185	-0.047

Note: *, **, and *** indicate significance levels of 10%, 5%, and 1%, respectively.

Considering the model diagnostics, the specification with both time and spatial fixed effects is preferred, as it shows the highest explanatory power (R-squared, Log-likelihood) along with the lowest AIC and residual variance. Therefore, I focus on this model for interpretation and occasionally refer to other specifications for comparison.

Across all the SDM specifications, direct and indirect effects of clinker production on NO_2 pollution are significant. That means clinker production not only affects pollution locally, but also that pollution crosses regional boundaries. More precisely, a one percent increase in clinker production within a given NUTS-3 region raises local NO_2 levels by 0.005%, reflecting the direct effect of clinker production. The spillover effects of clinker production are even stronger: comparable rise in clinker production in neighboring regions increases NO_2 levels in the region by 0.021%. This result is consistent with Li et al. (2020), who report that cement production generates stronger spillover effects than direct effects across Chinese provinces.

In all specifications, both gdp in logarithmic form and its squared term are statistically significant, with coefficients -0.584 and 0.030 respectively. This indicates that the relationship between economic output and air pollution across German districts follows a 'U-shaped' pattern, which contrasts with the Kuznets's "inverted U-shape" hypothesis. The result is similar to the findings of Destek et al. (2018), who find "U-shaped" relationship between air pollution and economic growth for EU countries. Our finding means that pollution does not continuously fall as GDP rises in Germany. Within a given county, as GDP per capita increases over the study period, pollution first tends to fall, but beyond a threshold, further increases in GDP per capita are linked to higher pollution levels. In addition, another research studying EKC hypothesis for 401 counties in Germany by examining nitrogen surplus as an environmental pollutant and median monthly wage as an economic growth rejects the existence of an "inverted U-shaped" relationship (Castro and Petrick, 2023). The paper concludes that in Germany, economic growth has not mitigated the environmental damage caused by nitrogen surplus.

Both direct and indirect impact of population density on air pollution is positive and significant across all the specifications. A one percent increase in the number of people per square kilometer within a district raises NO_2 concentrations in that district by about 0.19 percent, while a one percent increase in population density in neighboring districts increases local NO_2 concentrations by approximately 0.18 percent. There is a various literature (Wrightson et al., 2025; Borck and Schrauth, 2021) studying the relationship between population density and air pollution and the results are consistent that that higher population density is associated with higher environmental pollutants.

Another significant variable for NO_2 pollution is the industrial structure of the regions. Across all model specifications, the direct impact of industrial activity on NO_2 concentrations

is positive and statistically significant, with estimated coefficients ranging from 0.001 to 0.002. That means a one percentage point increase in the proportion of industrial value-added increases air pollution by 0.1%. These findings align with Li et al. (2018) who document that industrial activities increase air pollution. I also tested another measure for the structure of the economy, which is the share of tertiary (service) sector in the economy. Unsurprisingly, I got a negative significant coefficient (-0.001), reflecting that having higher share of service sector, in comparison to the industrial activities, reduces pollution.

As expected, diesel and petrol cars increase air pollution in the regions. An increase of one percent in the number of petrol and diesel cars per 1,000 inhabitants raises NO_2 concentrations in the same district by about 0.12 percent. Particularly, the role of diesel cars in creating NO_2 concentrations is discussed in the literature. Evidence from Norway shows that among passenger cars diesel cars account for the highest contribution to total road traffic NO_x emissions (47.9%), followed by petrol cars (4.9%), while other vehicle types contribute only marginally (Wærsted et al., 2022). Given this substantial difference in emission profiles, I re-estimated the model to include only diesel cars instead of both petrol and diesel. I expected even higher coefficient given that diesel cars pollute far more than petrol cars. However, the estimated effect remained similar (0.11). This result can be explained by the high correlation between diesel and petrol car ownership (0.95), meaning that regions with more diesel cars also tend to have more petrol cars, and vice versa.

Another transportation-related variable, traffic accidents, shows positive direct and spillover effects in two specifications but loses significance in the main specification. This may indicate that traffic accident data do not adequately capture traffic volume. Perhaps, with more direct measures of traffic, such as traffic counts or road congestion data, the result could be more robust.

According to the estimations, a higher share of employees in knowledge and research-intensive industries is associated with lower levels of air pollution, as reflected in the negative direct (-0.002) and indirect (-0.008) effects. This finding is expected, as regions with a stronger concentration of R&D-intensive sectors tend to adopt cleaner technologies. If data on R&D expenditures at the NUTS-3 level were available, the results could potentially be even stronger.

Another variable expected to reduce pollution in the NUTS-3 regions is the share of newly constructed residential buildings equipped with renewable heating systems. In the main model, the spillover effects of this variable are not significant, while the direct impact is significant at the 10 percent level. A more robust effect might be observed if data were available on the total share of residential heating supplied from renewable sources. Since the current

measure refers only to newly constructed buildings, it may not adequately capture the total use of renewable energy in the residential sector.

The direct impact of wind speed on air pollution is robust across all model specifications. As expected, higher wind speeds reduce pollutant concentrations within a region. Quantitatively, a one percent increase in wind speed lowers NO_2 concentrations by about 0.16 percent. However, no significant spillover effects are observed.

The spatial autoregressive coefficient, rho, is estimated at 0.73, indicating spatial correlation of NO_2 concentrations across NUTS-3 districts. This implies that air pollution levels in one district are strongly influenced by pollution in neighboring districts, which was also observed by Moran's I.

7. Robustness Check

7.1. Alternative Spatial Weight

As discussed, in the main specification, queen based spatial weight matrix is used. In this section, I re-estimated the Spatial Durbin Model using an inverse-distance spatial weights matrix. The table below reports the results.

Table 4. SDM estimates with inverse distance spatial weight matrix

	X	W*X	DE	IE	TE
asinh(Clinker)	0.005***	0.016*	0.007***	0.086**	0.093***
lngdp	-1.237***	0.524***	-1.302***	-1.618	-2.920**
$lngdp^2$	0.061***	-0.024***	0.064***	0.089	0.153**
lnPopDens	0.198***	-0.054***	0.207***	0.359***	0.566***
Ind	0.001***	0.0004	0.001***	0.006	0.007
lnCars	0.135***	-0.352***	0.121***	-1.089**	-0.968*
lnTraffic	-0.008	-0.062**	-0.015	-0.311**	-0.326**
Rd	-0.002***	-0.005***	-0.002***	-0.024***	-0.027***
RenHeat	-0.001***	-0.0004	-0.001***	-0.004**	-0.005***
ln(Wind)	-0.114***	0.096**	-0.119***	0.059	-0.061
ρ	0.751***				
R-squared	0.906				
Adj. R-squared	0.903				
$Sigma^2$	0.009				
Log-likelihood	3906.421				
AIC	-7705.41				
BIC	-7381.59				

Note: *, **, and *** indicate significance levels of 10%, 5%, and 1%, respectively. X and W*X columns present coefficients for explanatory variables and their spatial lags, respectively. DE, IE and TE stand for direct effect, indirect effect and total effect, respectively. Both time and spatial fixed effects are included.

Overall, the SDM estimates are consistent using both queen contiguity and inverse distance spatial weight matrices. Similarly, we have 'U-shape' relationship between economic output and pollution. In both cases, population density, proportion of industrial value added,

and the number of passenger cars with petrol and diesel engines increase air pollution. On the other hand, share of employees in R&D industries, the percentage of completed new residential buildings with renewable heating energy and wind speed reduce NO_2 concentrations.

The magnitude of the direct and indirect effects of clinker production is larger than in the previous model result, which can be attributed to the broader definition of neighbors in this specification. Basically, based on this model, a one percent increase in clinker production raises local NO_2 levels by 0.007% (previously 0.005%), and a one percent rise in neighboring regions increases NO_2 levels in the region 0.09% (previously 0.02%).

According to the model diagnostics, the SDM with distance-based weights underperforms relative to the queen contiguity specification, showing a lower adjusted R^2 and log-likelihood, as well as higher AIC and BIC values.

7.2. Alternative Model Specifications

As the next robustness check, in the next table I show the results of Spatial Durbin Error Model (SDEM) estimated with two spatial weights matrices. The difference is that SDEM does not include a spatial lag of the dependent variable. Instead, it captures spatial dependence through a spatially correlated error term.

Table 5. SDEM estimates with two spatial weight matrices

	Under W1 (queen based)		Under W2 (inverse distance-based)	
	X	W*X	X	W*X
asinh(Clinker)	0.004***	0.009***	0.006***	0.026***
lngdp	-0.482**	-0.454***	-1.111***	-0.210
$lngdp^2$	0.025**	0.026***	0.054***	0.007
lnPopDens	0.193***	0.086***	0.208***	0.146***
Ind	0.001***	0.0003	0.001***	0.002
lnCars	0.178***	0.298***	0.201***	0.278*
lnTraffic	0.014	-0.069**	-0.017	-0.181***
Rd	-0.002***	-0.002*	-0.002***	-0.008***
RenHeat	-0.0004**	-0.001***	-0.001***	-0.004***
ln(Wind)	-0.217***	0.058	-0.151***	0.082
lambda (λ)	0.833***		0.826***	
R-squared	0.864		0.887	
Adj. R-squared	0.860		0.883	
Sigma2	0.013		0.010	
Log-likelihood	4145.039		3856.696	
AIC	-8174.08		-7597.39	
BIC	-7850.25		-7273.56	

Based on the R documentation, the function impactspar() can not be used to get direct and indirect for 'sdem' and 'slx' models; instead summary() method is used to present the spatial impacts.

The SDEM results show that clinker production has a positive direct impact on air pollution, with an estimated effect of 0.004 under W1 and 0.006 under W2. These values are slightly lower than those obtained from the SDM specification (0.005 under W1 and 0.007

under W2). This model also confirms the presence of spatial spillovers; a one-percent increase in clinker production in neighboring regions raises local NO2 concentrations by 0.009% under W1 and 0.026% under W2. The results for other variables are consistent with SDM estimates.

Finally, I summarize the direct and indirect effects of clinker production on air pollution across all model specifications. Here I also include SAR and SEM model, with the full estimation outputs reported in the Appendix. All models are estimated with both time and spatial fixed effects under 2 spatial weight matrices.

Table 6.1. Model results for clinker production under W1

	SAR	SEM	SDM	SDEM
X	0.004***	0.002**	0.003***	0.004***
W*X			0.003***	0.009***
DE	0.005***		0.005***	
IE	0.004***		0.021***	
TE	0.009***		0.026***	
$pho(\rho)$	0.516***		0.731***	
lambda (λ)		0.907***		0.833***
R-squared	0.893	0.767	0.906	0.864
Adj. R-squared	0.891	0.761	0.903	0.860
Sigma2	0.01	0.022	0.009	0.013
Log-likelihood	4030.368	4023.052	4178.012	4145.039
AIC	-7964.74	-7950.1	-8240.02	-8174.08
BIC	7696.74	-7682.11	-7916.19	-7850.25

Note: *, **, and *** indicate significance levels of 10%, 5%, and 1%, respectively.

Table 6.2. Model results for clinker production under W2

	SAR	SEM	SDM	SDEM
X	0.006***	0.005**	0.005***	0.006***
W*X			0.016***	0.026***
DE	0.006***		0.007***	
IE	0.023***		0.086***	
TE	0.029***		0.093***	
$pho(\rho)$	0.789***		0.751***	
lambda (λ)		0.907***		0.826***
R-squared	0.827	0.891	0.906	0.887
Adj. R-squared	0.823	0.889	0.903	0.883
Sigma squared	0.02	0.01	0.009	0.010
Log-likelihood	3711.219	3629.361	3906.421	3856.696
AIC	-7326.44	-7162.72	-7705.41	-7597.39
BIC	-7058.44	-6894.73	-7381.59	-7273.56

Note: *, **, and *** indicate significance levels of 10%, 5%, and 1%, respectively.

Table 6 shows that across all model specifications and weighting schemes (queen contiguity and distance-based), clinker production increases air pollution, both through direct local effects and through spillover effects on neighboring districts.

Based on the model diagnostics, the SDM provides the best overall specification. The SDM outperforms alternative models in terms of fitness, with the highest R^2 (0.906) and adjusted R^2 (0.903), the lowest error variance (σ^2)and the strongest log-likelihood value (4178.012). It also achieves the lowest AIC (−8240.02) and BIC (−7916.19), indicating that the model's additional complexity is statistically justified.

7.3. Heterogeneity Analysis

Alternatively, following the findings of Wang et al. (2017), who report that effective spillover distances of industrial emissions are up to 56 km, I created buffer zones of 60 km around each cement plants and included those regions in the estimation. I estimated a Spatial Durbin Model using only the NUTS-3 regions that intersect with the 60 km clinker plant buffer zones. Table 7 summarizes the estimation results. In the map below, created buffer zones and corresponding regions are shown.

Figure 4. Clinker Plants and buffer zones (60km) around them

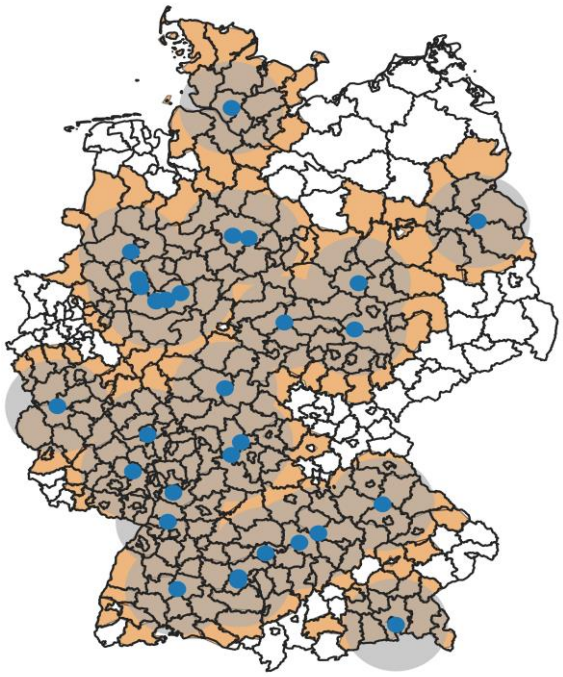

- Clinker plants are shown by blue points, and their 60 km buffer zones are depicted by grey circles.
- NUTS-3 regions intersecting with at least one buffer zone are highlighted in orange.
- The map was created in QGIS using Eurostat NUTS-3 boundaries and clinker plant location data by VDZ.
- Number of NUTS-3 regions in the buffered zones is 293.

Table 7. Estimation results of SDM for NUTS-3 regions within buffer zones

	Under W1 (queen based)			Under W2 (inverse distance-based)		
	DE	IE	TE	DE	IE	TE
asinh(Clinker)	0.006***	0.021***	0.027***	0.008***	0.074**	0.081**
lngdp	-0.780**	-0.851	-1.623*	-1.004***	0.632	-0.373
$lngdp^2$	0.040**	0.051	0.089*	0.050***	0.007	0.056
lnPopDens	0.211***	0.167***	0.377***	0.225***	0.178**	0.403***
Ind	0.002***	0.003	0.005*	0.003***	0.015**	0.017***
lnCars	0.207***	0.017	0.223	0.203***	-1.808***	-1.606***
lnTraffic	0.010	-0.108	-0.102	-0.018	-0.493***	-0.511***
Rd	-0.003***	-0.009**	-0.012***	-0.004***	-0.029***	-0.033***
RenHeat	-0.001***	-0.002**	-0.003***	-0.002***	-0.006***	-0.007***
ln(Wind)	-0.092***	0.185**	0.101	-0.075***	0.362**	0.287***
ρ			0.689***	0.693***		
R-squared	0.890			0.890		
Adj. Rsquared	0.886			0.886		
Sigma squared	0.009			0.009		
Log-likelihood	3047.443			2890.256		
AIC	-5990.89			-5676.51		
BIC	-5716.54			-5402.17		

Note: *, **, and *** indicate significance levels of 10%, 5%, and 1%, respectively

Based on Table 7, SDM estimated for NUTS-3 regions within a 60 km buffer zones, produces the same indirect effect of clinker as the baseline model (0.021), while the direct effect is slightly larger (0.006 compared to 0.005). When the inverse distance-based weight matrix is used, the direct impact of clinker production is estimated at 0.008, while the indirect impact is 074. Direction and significance of the relationships for all other variables are the same as the initial model. Full model specifications can be found in Appendix.

8. Discussion

Externalities, defined as the unintended costs or benefits of an activity borne by third parties, are a central source of market failure. While initial studies emphasized the economic and social dimensions of externalities, the focus has gradually shifted toward environmental externalities (Radukić and Perović, 2019).

In this paper, I examined the regional externalities of clinker production by analyzing its spatial spillover effects on air pollution across the NUTS-3 region. The results confirm the existence of environmental externalities: clinker plants do not only cause pollution in their host regions, but pollution effects also extend to neighboring districts. These findings suggest that effective mitigation policies for air pollution necessitate coordinated and joint governance, as air pollution is not confined to local boundaries.

Another interesting finding is the ‘U-shaped’ relationship between economic growth, measured by GDP per capita, and air pollution, measured by the average NO2 concentrations in the air. Halkos (2011) identified an ‘N-shaped’ relationship between economic growth and

pollution for 32 countries, including Germany. It is possible that Germany is currently situated in the 'U-shaped' segment of this broader 'N-shaped' trajectory. However, further research is required to confirm this dynamic.

Our findings show that population density has a significant impact on air pollution, which highlights the role of urban planning. In addition, the paper shows that how vehicle fleet composition is important for air pollution. Transitioning from diesel and petrol vehicles to low-emission alternatives can yield pollution reductions.

Beyond the factors that worsen air quality, the analysis shows that a higher share of employment in knowledge and research-intensive industries is associated with lower pollution levels. Similarly, the share of renewable heating systems in newly constructed houses shows a significant association with lower air pollution, although only at the 10% significance level. Incorporating a more direct measure of regional investment in R&D activities and renewable energy use by households could potentially strengthen the results.

Lastly, the analysis indicates that meteorological conditions also influence air quality. In particular, wind contributes to the dispersion of pollutants, reducing air pollution in the region. This underlines the importance of accounting for meteorological factors when analyzing air pollution dynamics.

9. Conclusion

This study examined the spatial spillover effects of clinker production on air pollution in Germany. Using panel data covering 393 counties for the period 2018–2022, the analysis employed the Spatial Durbin Model (SDM) as the main specification. The results provide clear evidence of regional environmental externalities, showing that clinker plants generate pollution impacts that extend beyond the regions in which they are located.

Bibliography

Aihounton, G.B. and Henningsen, A., 2021. Units of measurement and the inverse hyperbolic sine transformation. The Econometrics Journal, 24(2), pp.334-351.

Angelova, D. and Lupio, N.B., 2020. Constructing a meteorological indicator dataset for selected European NUTS 3 regions. Data in brief, 31, p.105786.

Anselin, L., 1988. Spatial econometrics: methods and models (Vol. 4). Springer Science & Business Media.

Bellemare, M.F. and Wichman, C.J., 2020. Elasticities and the inverse hyperbolic sine transformation. Oxford Bulletin of Economics and Statistics, 82(1), pp.50-61.

Bivand, R.S., Pebesma, E.J. and Gomez-Rubio, V., 2008. Applied spatial data analysis with R. New York, NY: Springer New York.

Borck, R. and Schrauth, P., 2021. Population density and urban air quality. Regional Science and Urban Economics, 86, p.103596.

Castro Campos, B. and Petrick, M., 2023. Nitrogen surplus displays a spurious Environmental Kuznets Curve in Germany. German Journal of Agricultural Economics (GJAE), 72(2), pp.91-100.

CEMBUREAU, 2024. The story of cement manufacture. Brussels: CEMBUREAU – The European Cement Association

Chen, J., Zeng, J., Shi, C., Liu, R., Lu, R., Mao, S. and Zhang, L., 2019. Associations between short-term exposure to gaseous pollutants and pulmonary heart disease-related mortality among elderly people in Chengdu, China. Environmental Health, 18(1), p.64.

Dai, Y.H. and Zhou, W.X., 2017. Temporal and spatial correlation patterns of air pollutants in Chinese cities. PloS one, 12(8), p.e0182724.

Destek, Mehmet Akif, Recep Ulucak, and Eyup Dogan, 2018. "Analyzing the environmental Kuznets curve for the EU countries: the role of ecological footprint." Environmental science and pollution research 25, no. 29 (2018): 29387-29396.

Ding, W. and Liu, J., 2023. Nonlinear and spatial spillover effects of urbanization on air pollution and ecological resilience in the Yellow River Basin. Environmental Science and Pollution Research, 30(15), pp.43229-43244.

EMEP/EEA, 2023. EMEP/EEA air pollutant emission inventory guidebook 2023: 2.A.1 Cement production. European Environment Agency. Available at: https://www.eea.europa.eu/publications/emep-eea-guidebook-2023

European Environment Agency (2022) Air quality data viewer – Average concentrations and health impact by country and region (NUTS). Available at: https://discomap.eea.europa.eu/App/AQViewer/index.html

Eurostat, 2025. NUTS - Nomenclature of territorial units for statistics, Overview - NUTS - Nomenclature of territorial units for statistics - Eurostat. Available at: https://ec.europa.eu/eurostat/en/web/nuts/overview.

Feng, T., Du, H., Lin, Z. and Zuo, J., 2020. Spatial spillover effects of environmental regulations on air pollution: Evidence from urban agglomerations in China. Journal of Environmental Management, 272, p.110998

Firdissa, B., Degefa, S., Mulugeta, E. and Sithole, D., 2024. Emissions from Ethiopian clinker-producing cement factories and their impact on community well-being. Discover Applied Sciences, 6(8), p.429.

German Informative Inventory Report, 2022. Available at: https://iir.umweltbundesamt.de/2022/sector/ippu/mineral_industry/cement_production/start

Halkos, G., 2011. Environment and economic development: determinants of an EKC hypothesis.

Heidelberg Materials, n.d. How cement is made. Available at: https://www.heidelbergmaterials.com/en/products-and-services/cement/how-cement-is-made

Jiang, Yixuan, Yue Niu, Yongjie Xia, Cong Liu, Zhijing Lin, Weidong Wang, Yihui Ge et al. "Effects of personal nitrogen dioxide exposure on airway inflammation and lung function." Environmental research 177 (2019): 108620.

Joint Research Center of European Commission. https://agri4cast.jrc.ec.europa.eu/dataportal

LeSage, J. and Pace, R.K., 2009. Introduction to spatial econometrics. Chapman and Hall/CRC.

Li, M., Li, C. and Zhang, M., 2018. Exploring the spatial spillover effects of industrialization and urbanization factors on pollutants emissions in China's Huang-Huai-Hai region. Journal of Cleaner Production, 195, pp.154-162.

Li, M., Zhang, M., Du, C. and Chen, Y., 2020. Study on the spatial spillover effects of cement production on air pollution in China. Science of The Total Environment, 748, p.141421.

Ma, Y.R., Ji, Q. and Fan, Y., 2016. Spatial linkage analysis of the impact of regional economic activities on PM2. 5 pollution in China. Journal of Cleaner Production, 139, pp.1157-1167.

Moran, P.A., 1950. Notes on continuous stochastic phenomena. Biometrika, 37(1/2), pp.17-23.

N'guessan, Y.G., Featherstone, A., Odeh, O. and Upendram, S., 2017. Choice of the empirical definition of zero in the translog multiproduct cost functional form. *Applied Economics Letters*, *24*(15), pp.1112-1120.

Ntziachristos, L., Samaras, Z., Kouridis, C., Samaras, C., Hassel, D., Mellios, G., Mccrae, I., Hickman, J., Zierock, H., Keller, M. and Rexeis, M., 2017. EMEP/EEA air pollutant emission inventory guidebook. PART B, 1.

Nwogu, F.U., Ubuoh, E.A., Kanu, C., Ogbaji, E.E. and Nwawuike, N., 2025. Effect of cement production processes on dry atmospheric chemistry in South-South Nigeria. Environmental Sciences Europe, 37(1), p.90.

Radukić, S. and Perović, D., 2019. Internalizing environmental externalities in cement industry: Case study for the republic of serbia and selected neighboring countries. Facta Universitatis, Series: Economics and Organization, (2), pp.379-392.

Rüttenauer, T., 2018. Neighbours matter: A nation-wide small-area assessment of environmental inequality in Germany. Social science research, 70, pp.198-211.

Salima, B.A. and Bellefon, M.D., 2018. Spatial autocorrelation indices. Handbook of Spatial Analysis: Theory Aplication with R, pp.51-68.

Schneider, M. and Behrouzi, D., 2023. Germany's net zero ambitions. International Cement Review, October, pp. 16-21.

Shekhar, S. and Xiong, H. eds., 2007. Encyclopedia of GIS. Springer Science & Business Media.

Shen, Y., Jiang, F., Feng, S., Zheng, Y., Cai, Z. and Lyu, X., 2021. Impact of weather and emission changes on NO2 concentrations in China during 2014–2019. Environmental Pollution, 269, p.116163.

Tao, C. and Yang, H., 2014. Spatial econometric model selection and its simulation analysis. Stat Res, 31, pp.88-96.

Thürkow, M., Banzhaf, S., Butler, T., Pültz, J. and Schaap, M., 2023. Source attribution of nitrogen oxides across Germany: Comparing the labelling approach and brute force technique with LOTOS-EUROS. Atmospheric Environment, 292, p.119412.

Wærsted, E.G., Sundvor, I., Denby, B.R. and Mu, Q., 2022. Quantification of temperature dependence of NOx emissions from road traffic in Norway using air quality modelling and monitoring data. Atmospheric Environment: X, 13, p.100160.

Wang, C., Du, X. and Liu, Y., 2017. Measuring spatial spillover effects of industrial emissions: a method and case study in Anhui province, China. Journal of Cleaner Production, 141, pp.1240-1248.

Wrightson, Samuel, Jamie Hosking, and Alistair Woodward. "Higher population density is associated with worse air quality and related health outcomes in Tāmaki Makaurau." Australian and New Zealand Journal of Public Health 49, no. 1 (2025): 100213.

Wu, X., Tian, Z., Kuai, Y., Song, S. and Marson, S.M., 2022. Study on spatial correlation of air pollution and control effect of development plan for the city cluster in the Yangtze River Delta. Socio-Economic Planning Sciences, 83, p.101213.

Zementwerke, V.D., 2023. Umweltdaten der Deutschen Zementindustrie—Environmental Data of the German Cement Industry 2023. VDZ: Düsseldorf, Germany

Zhao, C. and Wang, B., 2022. How does new-type urbanization affect air pollution? Empirical evidence based on spatial spillover effect and spatial Durbin model. Environment International, 165, p.107304.

Zhao, H., Cao, X. and Ma, T., 2020. A spatial econometric empirical research on the impact of industrial agglomeration on haze pollution in China. Air Quality, Atmosphere & Health, 13(11), pp.1305-1312.

Appendix

Table 1. SDM without fixed effects

Variable	Estimate	Std. Error	t value	Pr(>|t|)
(Intercept)	5.683**	2.541	2.237	0.0254
asinhclinker	0.003***	0.001	2.764	0.0058
Ind	0.001***	0.000	3.988	0.0001
lngdp	-0.920***	0.231	-3.979	0.0001
lngdp_squared	0.045***	0.011	4.083	0.0000
lnPopDens	0.178***	0.004	45.814	0.0000
lnCars	0.058**	0.024	2.389	0.0170
lnTraffic	0.028**	0.012	2.375	0.0176
Rd	-0.001*	0.000	-1.803	0.0716
RenHeat	-0.0001	0.000	-0.430	0.6674
lnWind	-0.176***	0.022	-8.158	0.0000
Wlag.asinhclinker	0.002	0.002	1.100	0.2717
Wlag.Ind	-0.0001	0.000	-0.391	0.6958
Wlag.lngdp	-0.333	0.439	-0.758	0.4485
Wlag.lngdp_squared	0.017	0.021	0.785	0.4326
Wlag.lnPopDens	-0.125	0.005	-26.331	0.0000
Wlag.lnCars	0.016	0.036	0.434	0.6645
Wlag.lnTraffic	0.018	0.018	1.008	0.3138
Wlag.Rd	-0.0001	0.001	-0.116	0.9076
Wlag.RenHeat	-0.001***	0.000	-2.671	0.0076
Wlag.lnWind	0.136***	0.029	4.679	0.0000
rho	0.889***	0.009	94.193	0.0000

Table 2. SDM with time fixed effects

Variable	Estimate	Std. Error	t value	Pr(>|t|)
asinhclinker	0.003***	0.001	2.942	0.0033
lngdp	-0.781***	0.233	-3.348	0.0008
lngdp_squared	0.038***	0.011	3.466	0.0005
lnPopDens	0.179***	0.004	45.856	0.0000
Ind	0.001***	0.000	3.302	0.0010
lnCars	0.077***	0.024	3.172	0.0015
lnTraffic	0.016	0.012	1.347	0.1780
Rd	-0.001***	0.000	-2.595	0.0095
RenHeat	-0.0002	0.000	-1.158	0.2470
lnWind	-0.150***	0.020	-7.579	0.0000
Wlag.asinhclinker	0.002	0.002	1.223	0.2217
Wlag.lngdp	0.015	0.051	0.286	0.7749
Wlag.lngdp_squared	0.001	0.003	0.403	0.6870
Wlag.lnPopDens	-0.105***	0.005	-21.933	0.0000
Wlag.Ind	-0.001*	0.000	-1.811	0.0703
Wlag.lnCars	0.064*	0.036	1.790	0.0735
Wlag.lnTraffic	-0.024	0.016	-1.478	0.1396
Wlag.Rd	-0.001*	0.001	-1.784	0.0746
Wlag.RenHeat	-0.0001	0.000	-0.484	0.6284
Wlag.lnWind	0.091	0.026	3.446	0.0006
rho	0.817	0.014	60.434	0.0000

Table 3. SDM with spatial fixed effects

Variable	Estimate	Std. Error	t value	Pr(>|t|)
(Intercept)	0.310	3.368	0.092	0.927
asinhclinker	0.003***	0.001	2.951	0.003
lngdp	-0.600**	0.247	-2.431	0.015
lngdp_squared	0.030**	0.012	2.542	0.011
lnPopDens	0.180***	0.004	44.883	0.000
Ind	0.001***	0.000	4.530	0.000
lnCars	0.093***	0.026	3.520	0.000
lnTraffic	0.037***	0.012	3.110	0.002
Rd	-0.001***	0.000	-3.364	0.001
RenHeat	-0.0003*	0.000	-1.897	0.058
lnWind	-0.207***	0.022	-9.484	0.000
Wlag.asinhclinker	0.003*	0.002	1.820	0.069
Wlag.lngdp	0.363	0.545	0.667	0.505
Wlag.lngdp_squared	-0.017	0.026	-0.634	0.526
Wlag.lnPopDens	-0.111***	0.008	-14.234	0.000
Wlag.Ind	0.000	0.001	0.046	0.963
Wlag.lnCars	-0.0320	0.061	-0.526	0.599
Wlag.lnTraffic	0.034*	0.019	1.781	0.075
Wlag.Rd	-0.001	0.001	-1.242	0.214
Wlag.RenHeat	-0.001***	0.000	-5.510	0.000
Wlag.lnWind	0.237***	0.033	7.209	0.000
rho	0.838***	0.013	66.656	0.000

Table 4. SDM with time and spatial fixed effects

Variable	Estimate	Std. Error	t value	Pr(>|t|)
asinhclinker	0.003***	0.001	3.70	0.000
lngdp	-0.512**	0.247	-2.08	0.038
lngdp_squared	0.026**	0.012	2.23	0.026
lnPopDens	0.179***	0.004	44.48	0.000
Ind	0.001***	0.000	3.05	0.002
lnCars	0.106***	0.027	3.94	0.000
lnTraffic	0.015	0.013	1.22	0.221
Rd	-0.001***	0.000	-3.32	0.001
RenHeat	-0.0002*	0.000	-1.84	0.065
lnWind	-0.168***	0.020	-8.25	0.000
Wlag.asinhclinker	0.003**	0.002	1.998	0.046
Wlag.lngdp	0.099	0.087	1.141	0.254
Wlag.lngdp_squared	-0.002	0.004	-0.511	0.610
Wlag.lnPopDens	-0.080***	0.008	-10.231	0.000
Wlag.Ind	-0.001	0.000	-1.515	0.130
Wlag.lnCars	-0.038	0.060	-0.626	0.531
Wlag.lnTraffic	-0.038**	0.018	-2.044	0.041
Wlag.Rd	-0.001	0.001	-1.466	0.143
Wlag.RenHeat	0.000	0.000	0.172	0.864
Wlag.lnWind	0.155***	0.030	5.231	0.000
rho	0.731***	0.019	39.108	0.000

Table 5.1. SAR model with time and spatial fixed effects under W1

Variable	Estimate	Std. Error	t value	Pr(>|t|)
asinhclinker	0.004***	0.001	4.111	0.000
lngdp	-0.186	0.265	-0.703	0.482
lngdp_squared	0.011	0.013	0.908	0.364
lnPopDens	0.171***	0.004	44.574	0.000
Ind	0.0005	0.000	1.591	0.112
lnCars	0.095***	0.029	3.243	0.001
lnTraffic	0.011	0.014	0.827	0.408
Rd	-0.002***	0.000	-3.194	0.001
RenHeat	-0.0004**	0.000	-2.338	0.020
lnWind	-0.0790***	0.016	-4.840	0.000
rho	0.516***	0.015	35.460	0.000

Table 5.2. SAR model with time and spatial fixed effects under W2

Variable	Estimate	Std. Error	t value	Pr(>|t|)
asinhclinker	0.006***	0.001	4.8735	0.000
lngdp	-1.445***	0.319	-4.5298	0.000
lngdp_squared	0.070***	0.015	4.6022	0.000
lnPopDens	0.211***	0.005	45.737	0.000
Ind	0.001***	0.000	3.9826	0.000
lnCars	0.216***	0.035	6.1616	0.000
lnTraffic	-0.005	0.016	-0.2793	0.780
Rd	-0.002***	0.001	-4.2802	0.000
RenHeat	-0.001***	0.000	-4.7704	0.000
lnWind	-0.038*	0.020	-1.9344	0.053
rho	0.789***	0.03	26.0280	0.000

Table 6.1. SEM with time and spatial fixed effects under W1

Variable	Estimate	Std. Error	t value	Pr(>|t|)
asinhclinker	0.002**	0.001	2.475	0.013
lngdp	-1.210***	0.215	-5.618	0.000
lngdp_squared	0.057***	0.010	5.636	0.000
lnPopDens	0.185***	0.004	46.853	0.000
Ind	0.001***	0.000	5.821	0.000
lnCars	0.121***	0.025	4.845	0.000
lnTraffic	0.031**	0.012	2.521	0.012
Rd	-0.001***	0.000	-3.310	0.001
RenHeat	-0.0001	0.000	-0.875	0.382
lnWind	-0.190***	0.021	-8.855	0.000
lambda	0.907***	0.012	76.369	0.000

Table 6.2. SEM with time and spatial fixed effects under W2

Variable	Estimate	Std. Error	t value	Pr(>|t|)
asinhclinker	0.005***	0.001	4.163	0.000
lngdp	-1.565***	0.329	-4.751	0.000
lngdp_squared	0.074***	0.016	4.758	0.000
lnPopDens	0.220***	0.005	45.477	0.000
Ind	0.002***	0.000	5.428	0.000
lnCars	0.245***	0.036	6.763	0.000
lnTraffic	-0.017	0.017	-0.992	0.321
Rd	-0.003***	0.001	-4.958	0.000
RenHeat	-0.001***	0.000	-4.433	0.000
lnWind	-0.036*	0.021	-1.719	0.086
lambda	0.895***	0.017	57.885	0.000

Table 7. SDM estimations for buffered zones under spatial weight 1 and 2

	Under W1 (queen based)		Under W2 (inverse-distance based)	
	X	W*X	X	W*X
asinh(Clinker)	0.004***	0.004**	0.006***	0.018**
lngdp	-0.735**	0.234**	-1.013***	0.906***
$lngdp^2$	0.036***	-0.008	0.049***	-0.032***
lnPopDens	0.199***	-0.082***	0.221***	-0.099***
Ind	0.002***	-0.001	0.002***	0.003
lnCars	0.206***	-0.139*	0.251***	-0.731***
lnTraffic	0.016	-0.048**	-0.006	-0.147***
Rd	-0.002***	-0.001	-0.003***	-0.007***
RenHeat	-0.001***	-0.0002	-0.002***	-0.001
ln(Wind)	-0.106***	0.135***	-0.083***	0.171***

I hereby confirm that the work presented has been performed and interpreted solely by myself except for where I explicitly identified the contrary. I assure that this work has not been presented in any other form for the fulfillment of any other degree or qualification. Ideas taken from other works in letter and in spirit are identified in every single case.

Date:

Signature: